This is a repository copy of *Ultrasonically assisted drilling in marble*.

White Rose Research Online URL for this paper:
http://eprints.whiterose.ac.uk/151346/

Version: Accepted Version

Article:

Ultrasonically assisted drilling in marble

N. Mikhailova [a],[*], P.Y. Onawumi [b], G. Volkov [a], I. Smirnov [a], M. Broseghini [c], A. Roy [b], Yu Petrov [a], V.V. Silberschmidt [b]

[a] *Saint Petersburg University, Universitetskaya nab 7/9, Saint Petersburg, 199034, Russia*
[b] *Wolfson School of Mechanical, Electrical and Manufacturing Engineering, Loughborough University, Loughborough, LE11 3TU, UK*
[c] *Department of Civil, Environmental and Mechanical Engineering, University of Trento, Via Mesiano 77, Trento, 38123, Italy*

A B S T R A C T

Ultrasonically assisted drilling (UAD) is a non-traditional machining process that employs the vibration of a cutting tool. It offers a better alternative and solution to the challenges of drilling marble using conventional drilling (CD) methods. Machining-induced damage in marble results in the rejection of parts. A significant force reduction is achieved when applying UAD in marble, therefore eliminating large craters created at the exit of the hole in CD, caused by the high force generated. This work presents original experimental results for both drilling techniques, and suggests an analytical model for UAD based on a combination of a contact-problem solution and an incubation-time approach. In the modelling, the problem of fracture at different scales was considered, solved by employing a principle of equal power. The predictions of the presented theoretical model for UAD were validated by comparison with the experimental data, demonstrating a good qualitative agreement.

1. Introduction

Marble is used widely in architectural building products, sculptures, landscape gardening and decorative pieces. In construction, marble is subjected to various machining processes, such as drilling, to facilitate the assembly of parts. Due to its brittle nature, such manufacturing is often accompanied by the formation of spalls, cracks and latent defects in a work piece, or even by failures, leading to a significant amount of rejected material. Consequently, a less damaging machining process is needed.

A method combining ultrasonic vibration with a conventional cutting motion was developed in the 1950s [1]. Applying vibration helps to stabilise the cutting tool, transforming a continuous process into a vibro-impact one, leading to improved cutting quality. Later, ultrasonic vibration was superimposed onto the drilling and turning processes [2,3]. Improvements related to the use of ultrasonically-assisted machining positioned it as very advantageous, compared to its conventional counterpart.

Ultrasonically assisted drilling (UAD) is a hybrid machining process in which high-frequency vibration is superimposed on the movement of a drill bit, typically in the axial direction. Investigations of UAD have demonstrated reductions in the levels of the cutting forces and significant enhancement of the surface quality of work pieces, compared to the conventional drilling (CD) process. In metals, UAD has prevented serious work hardening and the sticking of chips to the drilling tool, thus

---

improving hole circularity and permitting the drilling of metal plates without inducing strong deformations [4–6]. Azghandi et al. [7] performed a comparative study by applying different vibration amplitudes (at 10 μm and 15 μm) in UAD to the drilling of high-alloy steel versus using CD. They demonstrated an average thrust force reduction of 57% using UAD at an amplitude of 10 μm, with a further reduction to 62% for an imposed amplitude of 15 μm. Makhdum et al. [8] investigated the effect of UAD on carbon-fibre-reinforced plastics (CFRPs). An application vibration at 27.8 kHz produced an average thrust force reduction of up to 60% and a torque reduction in excess of 90%. In addition, the UAD of composite materials resulted in a decrease in their delamination [8,9].

Brittle materials have also been considered in studies of UAD. Babitsky et al. [10] analysed UAD for glass, using a torsional transducer. Their results showed a significant force reduction in the axial direction, with a decrease in the damaged area when compared to CD. Recently, a study on the drilling of stones using UAD at varied ultrasonic power showed a force reduction of 20% [11]. Thus, a thorough study on the drilling of marble is warranted, as there are various applications in which machinability improvements could prove beneficial.

It should be noted, however, that most previous works on UAD have been experimental, or based on finite-element modelling [3,12], while the theoretical description of such methods has received less attention. The theoretical modelling of UAD is generally based on fundamental kinematic models [13–15]. These models are based on the equations of motion that take into account the superimposition of macroscopic kinematics onto the tool with ultrasonic vibrations, aimed at predicting a material removal rate. Still, the studies by Qin et al. [16] and Liu et al. [17] can be highlighted. They introduced a physics-based model of a cutting force and its variation as a function of experimental input parameters, such as the size and number of diamond particles, the frequency and amplitude of vibration, the cutting speed and the feed rate. The derivation of such models for the cutting force allows optimisation of the process of UAD based on a variation of the input parameters.

However, these works have not significantly considered the approaches of dynamic fracture mechanics and continuum mechanics under dynamic loads, and material processing is associated with the fracture of the surface layer. Consequently, an accurate and predictive description of the effect of ultrasonic vibrations on the drilling process of a particular material can only be given by taking into consideration the temporal characteristics of the fracture processes. For example, in Ref. [18], it was shown that the dependence of the cutting force on the material feed rate can be determined by introducing the minimum threshold fracture energy and the characteristic (incubation) fracture time.

Thus, UAD models are useful tools for elucidating the fundamental principles of complex mechanical techniques, allowing the prediction of such parameters as cutting forces, and playing a crucial role in the successful application of the process and its optimisation. In this study, a comparative experiment, involving the drilling of marble using two drilling techniques — CD and UAD — was performed. To find the optimal drilling parameters for marble, the tests were carried out using various types of drill bits. A dependence on the level of thrust force and torque on the drilling speed was considered for each drill bit for both the CD and UAD methods. The present work also developed a new analytical model for the calculation of thrust forces operating during the UAD process. The model is based on a combination of a fracture-mechanics approach, using a problem of contact mechanics [18,19]. The incubation-time approach [20,21] was employed to determine a threshold fracture energy that would allow the prediction of the cutting force in UAD. This study also considered the length scale of the fracture. The principle of equal power [22,23] was applied to derive material properties from the length scale of the fracture required by the model, using experimental tests with a split Hopkinson pressure bar (SHPB) [24,25]. The theoretical predictions are discussed, and validated by comparison with experimental data for the case study of marble.

2. Experimental procedure

2.1. Methods and materials

The experimental drilling studies were conducted on a universal Harrison M-300 lathe, as shown in Fig. 1, which was effectively modified to integrate a Langevin-type piezoelectric transducer [8], mounted in its three-jaw universal chuck, with
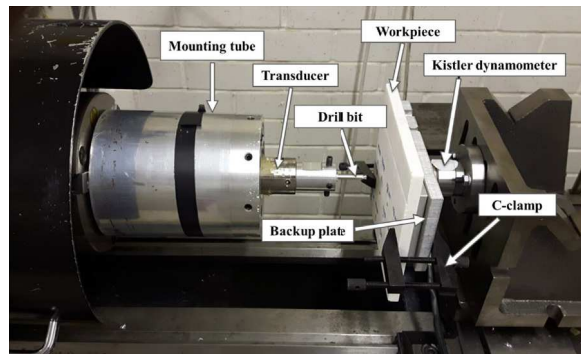

Fig. 1. Experimental setup.

Table 1
Mechanical and physical properties of marble.

Property	Unit	Value
Density (ρ)	kg/m^3	2870
Elasticity modulus (E)	GPa	16
Poisson's ratio (v)	—	0.26
Static tensile strength (σ_t)	MPa	3.9
Tensile incubation time of fracture (τ_t) [20]	μs	135
Critical fracture toughness (K_{lc})	MPa$\sqrt{\mathrm{m}}$	0.39

Table 2
Tool descriptions.

	Core drill bit	CYL-3 masonry drill bit	HSS jobber drill bit
Diameter	Inner 4.0 mm Outer 6.0 mm	3.0 mm	3.0 mm
Working length	5.3 mm (shank size)	40.0 mm	33.0 mm
Total length	55.0 mm	70.0 mm	61.0 mm
Material	Stainless steel with abrasive diamond coating	Stainless steel	Cobalt high-speed steel with TiN coating

Fig. 2. Drilling tools used: (a) core drill bit; (b) masonry drill bit; (c) HSS jobber drill bit.

a maximum power rating of 106.6 W and a maximum rotational speed of 2500 rpm. The transducer was composed of piezoelectric ceramics rings, a front mass, a backing mass and a central bolt. A drill bit was fixed to the front mass using a modified design to maximise the amplitude in the axial mode of vibration.

A two-component dynamometer (Kistler 9345b) was placed on the cross slide of the lathe, fixed on an angle plate, to measure the thrust force and torque during the drilling process. Force data measured by the dynamometer were obtained using charge amplifiers that converted and transmitted the data through an analogue/digital converter (Picoscope digital oscilloscope) connected to a computer. The marble sample was C-clamped onto the backing plate attached to the dynamometer.

A fine-grained (<200 μm) marble was selected as the reference material, owing to its homogeneous structure, to help in reducing fluctuations in the cutting force during the drilling process. Additionally, marble typically has a highly polished surface, making a damaged area easily noticeable. The experimental drilling was performed on square plates (305 × 305 × 10.5 mm) of this marble. The mechanical and physical properties of marble are given in Table 1.

The drilling was conducted using three different drill bits: a core drill of ⌀6 mm with diamond grit; a ⌀3 mm Bosch CYL-3 masonry drill bit; and a ⌀3 mm high-speed steel (HSS) jobber drill bit (Fig. 2). Details of the drilling tools are listed in Table 2. Vibrations were applied in the axial direction at the drill tip for the UAD experiments.

The first and second drill bits were designed for drilling brittle materials, such as concrete, so they were chosen to test on the marble. The 6-mm-diameter core drill bit was used because the 3-mm-diameter drill bit broke during the drilling experiment. The third drill bit is usually used for metal processing, and had deeper flutes and sharper edges than the previous two. This drill bit was chosen because it was thought that its sharp edges might reduce the damage in the vicinity of the drilling hole.

2.2. Experimental conditions

The drilling experiment was performed using a minimal constant feed rate set at 0.03 mm/rev, as a prior study had indicated that a low feed rate produced a better hole quality and finish [26]. To study the material behaviour and find the optimal drilling parameters using UAD, the experiments were carried out at a range of spindle speeds. The choice of the range

Table 3
Parameters of ultrasonic vibration used in UAD.

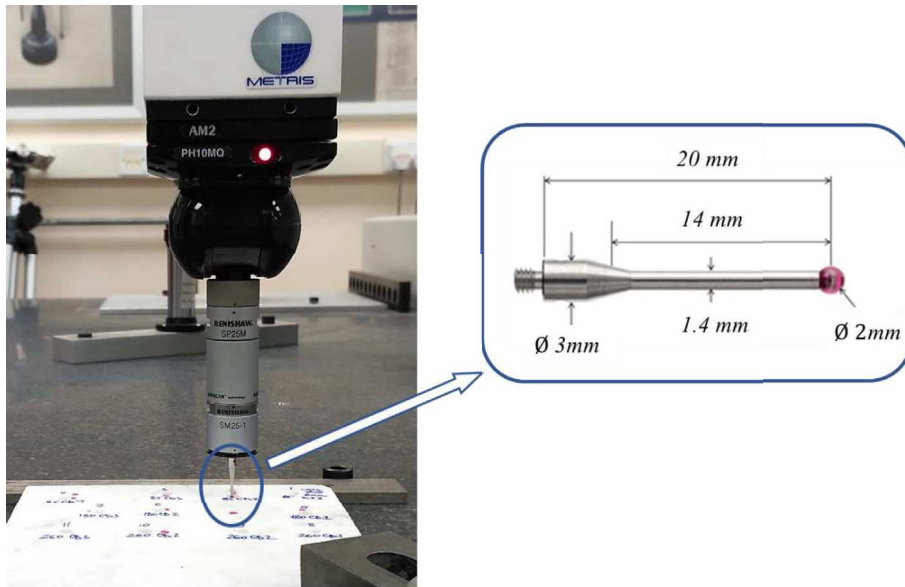|	Core drill bit	Masonry drill bit	HSS jobber drill bit
Frequency, kHz	25.91	37.4	37.9
Amplitude (peak-to-peak), μm	5.7	3.5	3.7

Fig. 3. Circularity measurement using a Metris LK Ultra 627134 CMM.

was made based on a study of different drilling speeds employed in marble with different strengths, which showed that lower-strength marble required lower speeds than higher-strength marble [26]. It is also worth noting that the setup allowed only a specific set of spindle speeds and feed rates, thus defining the experimental envelope.

The UAD experiments with the core drill bit provided stable results, so only three spindle speeds — 85, 180 and 260 rpm — were used. In the case of the masonry and jobber drill bits, the force and torque values depended on the speed; therefore, the range of spindle speed was wider, being from 40 to 800 rpm. Additionally, to investigate the unusual force and torque growth in UAD in the case of the jobber drill bit, the experiments with a feed rate from 0.03 to 0.06 mm/rev were conducted in increments of 0.01 mm/rev.

To measure the vibration amplitude at the drill tip during the UAD, a Polytec™ laser vibrometer (OFV-3001) was used, with the capability of measuring vibrations at a velocity of 10 m/s and a resolution of 0.08 μm/s. The levels of frequency and amplitude at the drill tip were tuned to the maximum free vibration during this process. The ultrasonic frequencies and peak-to-peak amplitudes applied in the UAD for each drill bit are presented in Table 3.

2.3. Surface metrology and damage analysis

A post-drilling analysis was conducted to assess the quality of the drilled holes obtained via the CD and UAD techniques. The holes were analysed to measure the diameter and circularity error, using a Metris LK Ultra 627134 coordinate-measuring machine (CMM), equipped with a Renishaw head with an analogue scanning probe PH10MQ SP25_1 and a Ø2 mm ruby ball stylus (product code A-5000-3603), as shown in Fig. 3. Hole measurements were taken at three different depths — 1, 5 and 8 mm from the entry face of the marble plate.

An Alicona Infinite Focus microscope, with a magnification of 5 ×, was used to measure the extent of damage induced by the drilling using both drilling techniques. The extent of the damage was analysed by assessing the depth and roughness of the crater.

3. Experimental results

3.1. Drilling with the masonry drill bit

The levels of thrust force and torque measured in CD and UAD with the masonry drill bit are shown in Fig. 4. The zero values at the beginning correspond to the absence of tool contact with the material (i.e. as the drill bit approached the sample). The initial penetration of the drill bit into the sample was characterised by a gradual increase in the thrust force and torque. Then, their values became (nearly) constant when the drill's cutting edges were in full engagement with the marble. The end of drilling corresponds to the drop in force and torque.

The measured signal was constant during the second stage of the UAD, but in the CD, a steady increase in the force and a torque jump at the end were observed. That growth led to spalling on the back side of the sample. This phenomenon may be associated with the accumulation of marble dust inside the drilled hole, increasing the friction and reducing the cutting
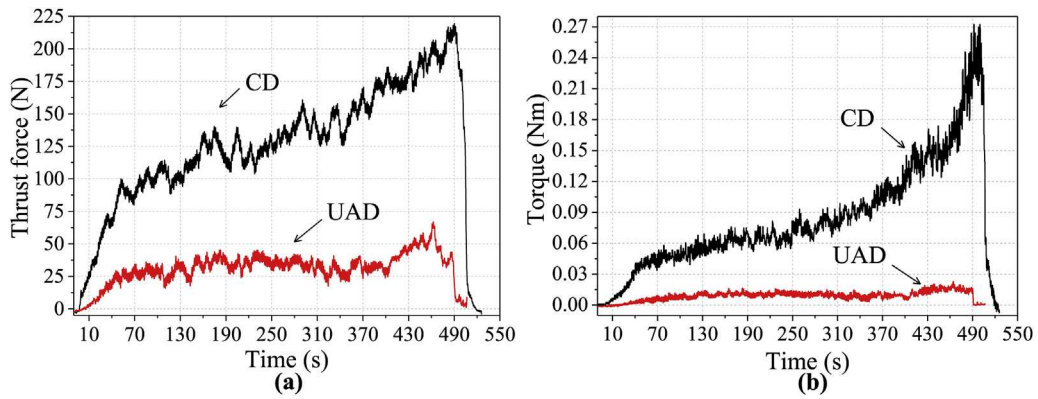
Fig. 4. Thrust force (a) and torque (b) in CD and UAD using a masonry drill bit (spindle speed 40 rpm, feed rate 0.03 mm/rev).
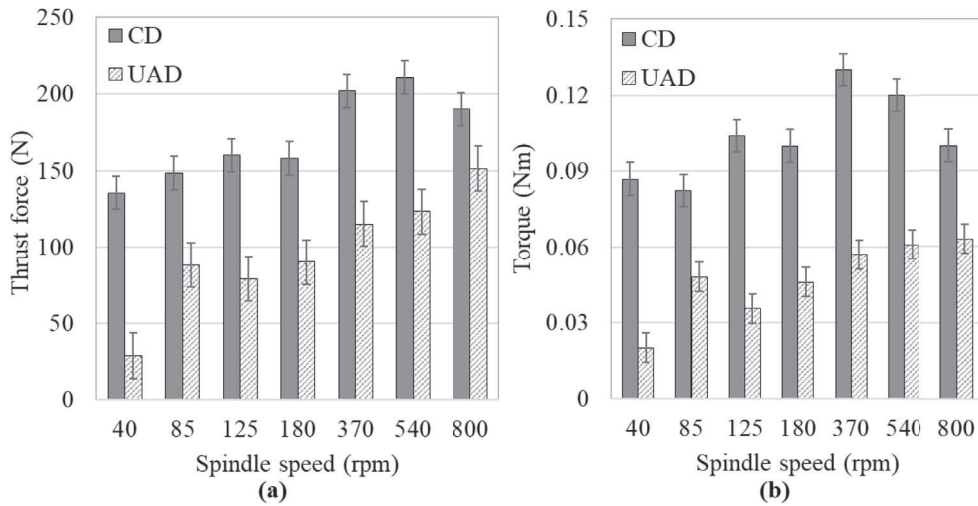

Fig. 5. Average thrust force (a) and torque (b) in UAD and CD using a masonry drill bit.

ability of the drill bit. In the UAD, thanks to the vibration, marble dust did not accumulate inside the hole. As a result, growth in the thrust force and torque were not observed.

The values of the thrust force and torque, averaged for each spindle speed, in the drilling tests using the masonry drill bit are given in Fig. 5. The thrust force increased with the speed, but at the maximum spindle speed, some decrease was observed. The torque with increasing speed reached a maximum at 370 rpm, and then started to decrease.

Comparison of the two drilling techniques revealed that the UAD contributed to a decrease in the thrust force and torque by an average of 45% and 54%, respectively. The most effective spindle speed was 40 rpm. In this case, the reduction was 79% for the thrust force and 77% for the torque, and their values were the lowest for the entire test range (Fig. 5).

3.2. Drilling with the HSS jobber drill bit

The sharper edges of the jobber drill bit contributed to an improvement in the cutting process, so the total values of the force and torque in the CD were less than with the masonry drill bit. There was also no definite trend in the thrust force and torque with increased cutting speed (Fig. 6); their values fluctuated. The exceptions were the experiments with the CD performed at a spindle speed of 800 rpm, where both the thrust force and the torque decreased by approximately twice that obtained at other spindle speeds.

The implementation of UAD for this type of drill bit was more effective than for the masonry drill bit. The extent of the reduction in the thrust force and torque averaged 80% and 93%, respectively, for all speeds, except at a spindle speed of 800 rpm. At this speed, the thrust force reduction was only 15%. This deterioration was associated with a sharp increase in the thrust force and torque at the end of the drilling process, as shown in Fig. 7.
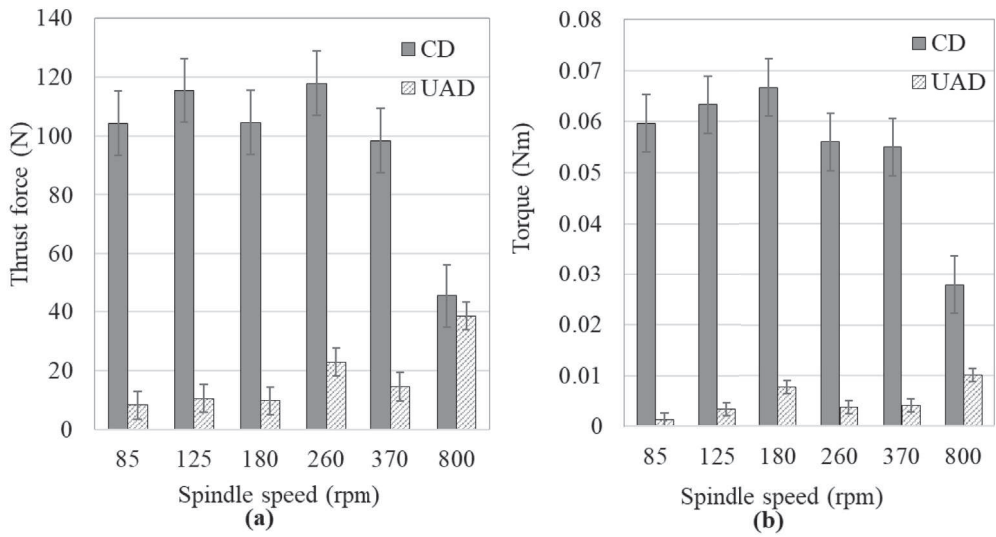
Fig. 6. Average thrust force (a) and torque (b) in UAD and CD using a jobber drill bit.
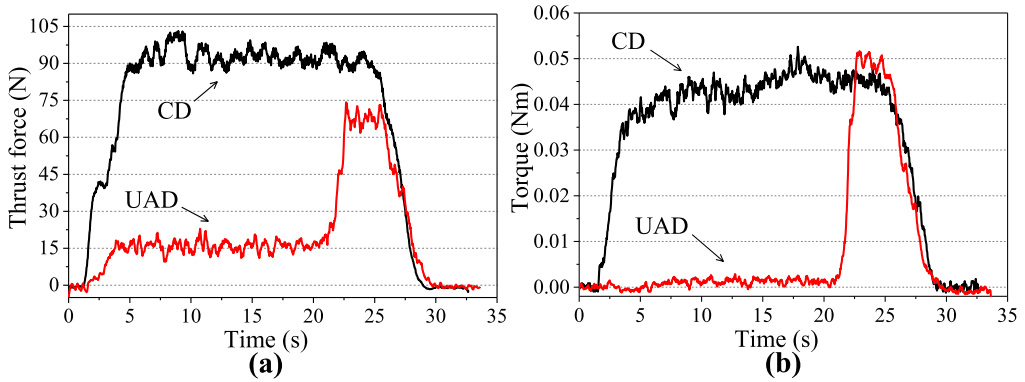

Fig. 7. Evolution of thrust force (a) and torque (b) in UAD and CD using a jobber drill bit (spindle speed 800 rpm, feed rate 0.03 mm/rev).
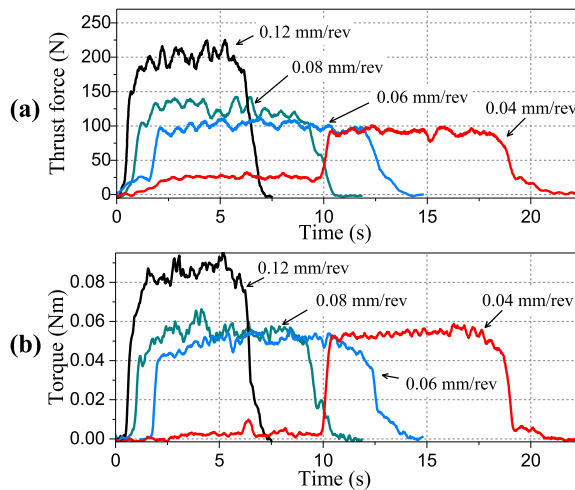

Fig. 8. Thrust force (a) and torque (b) in UAD using a jobber drill bit (spindle speed 800 rpm).
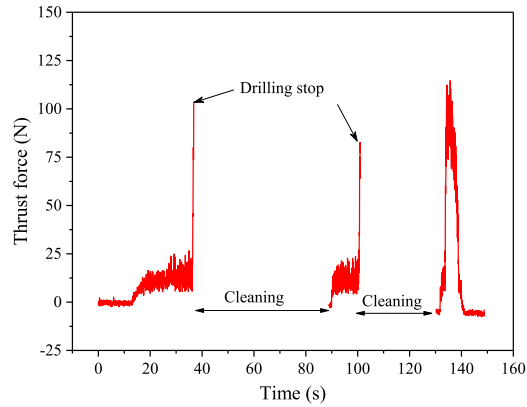
Fig. 9. Effect of cleaning marble dust from the jobber drill bit during UAD.

To investigate this atypical growth, a set of experiments was conducted at spindle speeds of 800 rpm, in which the feed rate was increased from 0.03 to 0.12 mm/min (Fig. 8). The results show that, with the increase in feed rate, the duration of the jump increased, as well as the amplitudes of the thrust force and torque, bringing them closer to the values obtained using CD. When the feed rate was greater than, or equal to, 0.08 mm/rev, a reduction in the initial stage did not occur, and the profiles of the thrust force and torque obtained from the UAD were identical to those measured in CD. Furthermore, similar tests were carried out at a lower speed of 370 rpm. These results showed that the same increase in thrust force and torque was present at feed rates of 0.04 mm/rev and higher.

This effect can be explained by the fact that this drill bit had deep flutes, which accumulated and compacted marble dust. This reduced the space available for vibration and, as a result, caused full contact between the material and the tool. Thus, the UAD effectively became CD, losing its vibro-impact feature and resulting in a sharp increase in the thrust force and torque. To test this assumption, another experiment was performed, where the drilling was stopped when the thrust force increased abruptly. At this point, the tool and drill hole were cleaned, and then drilling was continued. As seen in Fig. 9, after cleaning, the thrust force returned to a low level corresponding to UAD. After a second cleaning, the drilling was completed without stopping, as represented by the final peak in the force diagram (Fig. 9).

3.3. Comparison of drilling with the masonry and jobber drill bits

A comparison of the average thrust forces obtained from both drilling techniques, using the masonry and jobber drill bits, is depicted in Fig. 10. Thanks to the sharper edges of the jobber drill bit, the thrust force levels were lower than in the case of the masonry drill bit for both the UAD and CD. The thrust force values obtained for UAD with the masonry drill bit were close to those for the CD using the jobber drill bit. Moreover, at feed rates of 370 and 800 rpm, the thrust force in the UAD with the masonry drill bit exceeded the values from the CD with the jobber drill bit.

The greatest improvement in drilling the marble was achieved using UAD with the jobber drill bit. The thrust force did not exceed 23 N at spindle speeds of up to 370 rpm. Such a low force intensity makes marble drilling less damaging. However,
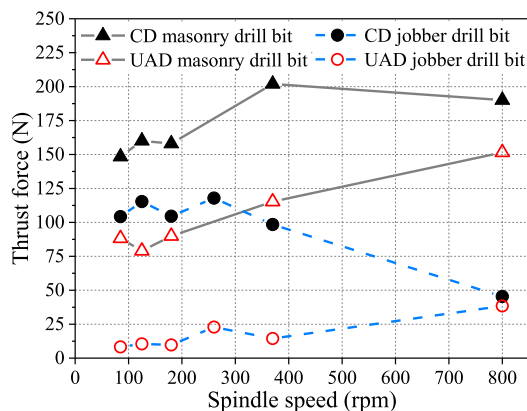

Fig. 10. Comparison of averaged thrust forces in CD and UAD using masonry and jobber drill bits.

UAD with the jobber drill bit at spindle speeds higher than 370 rpm led to dust compaction and the rapid loss of effective ultrasonic action.

3.4. Drilling with the core drill bit

3.4.1. Thrust force and torque analysis

The effect of the cutting process using the diamond core drill bit is shown in Fig. 11. In the CD, the thrust force exerted on the marble gradually increased as the drill penetrated the sample, with a maximum occurring towards the end of the run, reaching almost 400 N. In the final stage, when the material was too thin and weak to sustain the thrust force, the drill bit pushed out the marble material rather than drilling through it. Consequently, the drilling time was shorter than the duration needed to drill through the marble.

The reason for this increase in force in the CD was the accumulation of marble dust inside the core drill in the initial stage, without the possibility of its evacuation. This increased the friction and total cutting forces in the subsequent drilling. Ultrasonic vibration, in contrast, promoted the release of the dust. Moreover, in the UAD, the core drill cut the material along the drill edge, leaving small marble cylinders inside the bit (Fig. 12b), while in the CD, the marble dust entirely filled up the core drill (Fig. 12a).

Drilling the marble using the UAD method improved the cutting efficiency, in terms of reduced cutting forces, as shown in Fig. 13. This led to benefits such as diminished or eliminated damage to the material, longer tool life and a better surface finish, all of which would reduce the production costs. In this case, the UAD demonstrated its ability to reduce the stress imposed at the exit of the drilled hole, thereby reducing the dimensions of the cratering. Marble is naturally brittle. Consequently, the higher force induced by CD creates a larger crater at the exit, with the drill bit pushing out a fragment of marble rather than drilling all the way through it.

As the cutting speed increased, the thrust force decreased using CD. At 85 rpm, a higher force was required to drill through the material, with an average thrust force of 252 N, while the UAD reduced the thrust force to 6 N. Further increases in speed in the UAD led to a slight increase in thrust force and low-level fluctuations in the torque. In the CD tests, the averages of the thrust force and torque decreased with increasing cutting speed.
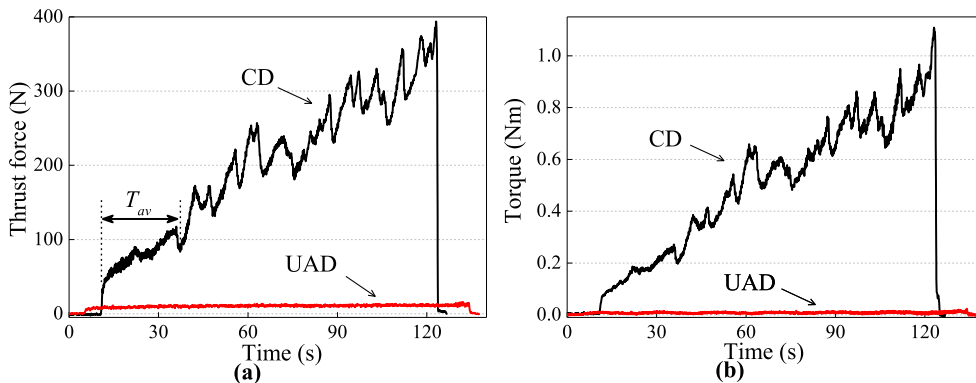

Fig. 11. Thrust force (a) and torque (b) in UAD and CD using a core drill bit (spindle speed 180 rpm, feed rate 0.03 mm/rev; T_{av} is an averaged period [see Section 4]).
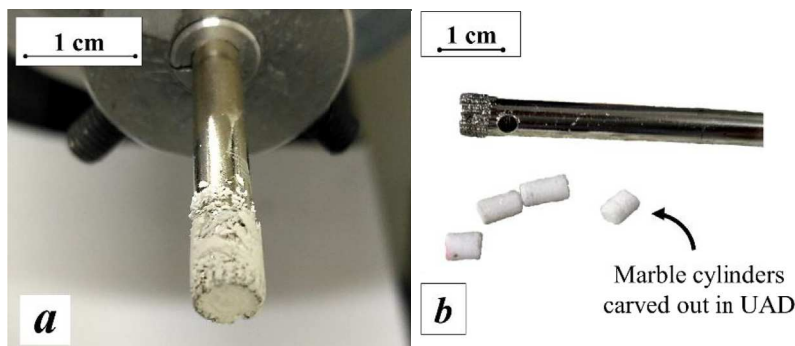

Fig. 12. (a) Marble dust compaction inside the core drill bit after CD. (b) Marble cylinders formed inside the core drill after UAD.
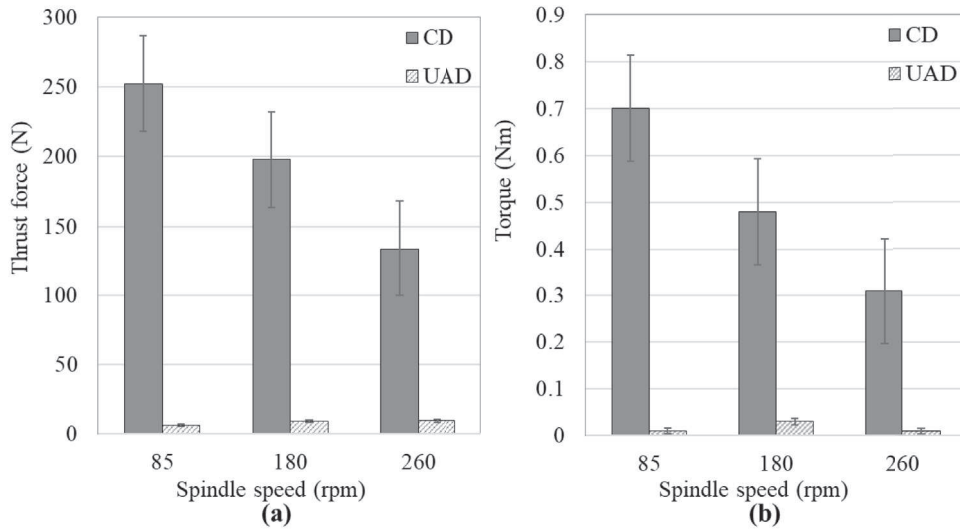
Fig. 13. Comparison of average thrust force (a) and torque (b) in CD and UAD in marble for different spindle speeds.

Evidently, the UAD-induced force reduction was significant when compared to the CD; for example, this was 98% at a spindle speed of 85 rpm. This could be related to the intermittent separation action. Similar force behaviour was observed in drilling CFRP, where a 60−80% force reduction was achieved [8]. UAD is effective because the tool disengages from the material in each vibratory cycle during the drilling process. It is apparent that UAD is able to produce superior-quality holes to CD, even at higher cutting speeds, as the forces required for the UAD are significantly lower.

3.4.2. Hole circularity and diameter

The dimensions of a drilled hole are an important factor in engineering tolerance. After the completion of the experiments, measurements of the hole diameters and circularity errors were carried out, employing the CMM. A typical scan of the surface inside the drill hole at one of the depth levels (see Section 2.3) is depicted in Fig. 14. The error in circularity was calculated as the sum of the maximum peak (RoNp) and the maximum trough (RoNv) values, with a zero value corresponding to a perfect circle.

The diameter and circularity of the drilled holes were measured for both the CD and UAD methods, as shown in Fig. 15. The results demonstrate that the hole diameter more closely corresponded to the core drill bit diameter of 6 mm using CD rather than UAD. This is likely associated with vibration in the torsional directions. Hole circularity was better using UAD than CD. At 85 rpm, hole circularity was relatively poor from CD, whilst the UAD produced better hole circularity at most cutting speeds. Both drilling methods produced holes that were larger than the nominal drill diameter of 6 mm. This can be attributed to
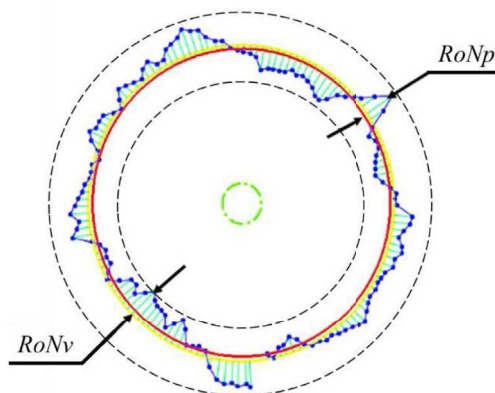

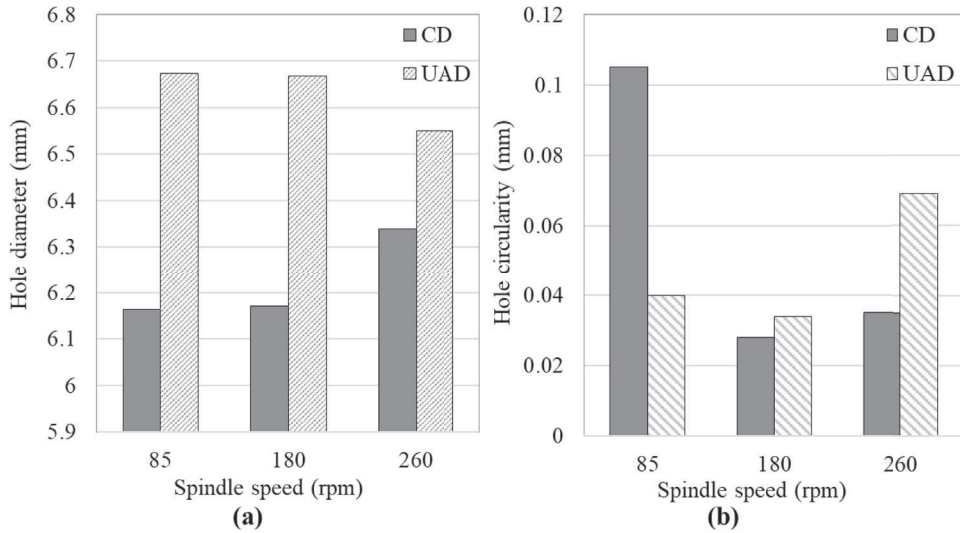Fig. 14. Contour of hole drilled in marble.

Fig. 15. Hole analysis after CD and UAD at different spindle speeds. (a) hole diameter, (b) hole circularity.

'chatter' during the machining procedures, with vibrations affecting hole size. Generally, it was observed that UAD resulted in better hole quality than CD.

3.4.3. Drilling-induced damage

Areas typifying damage, in 3D profile, are shown in Fig. 16. A comparative analysis is presented to demonstrate the relative quality of the holes produced using CD versus UAD. Our investigation showed significant improvements in hole quality using UAD over CD. The lower forces produced by the UAD resulted in a reduction in the damage incurred during the drilling process. The higher stress initiated in the samples by CD exceeded the sample strength, with the drill breaking through the material at the hole exit, creating a crater and causing significant damage to the marble. The UAD successfully reduced such drilling-induced damage. Apparently, UAD is preferable for producing high-quality holes in marble.

Measurements of the craters (Fig. 17) demonstrated that the damage using UAD was reduced by 80% at the slowest speed, and by 46% at the highest speed. Using CD, the damage incurred was not only limited to the crater; an internal damage cloud was observed around the drilled hole. However, it should also be noted that, in the CD, the crater depth decreased linearly with increasing speed, while in the UAD, it slowly increased. Still, UAD can be employed at higher speeds, whilst inducing lower damage in the marble.

In order to estimate the damage caused by the drilling process, a damaged area factor (F_d) was calculated as the ratio of the maximum diameter (D_{max}) of the damaged area to the nominal diameter (D_{nom}) of the drill:

$$F_d = \frac{D_{max}}{D_{nom}}.$$

An example of a damaged area on the back surface of a sample is presented in Fig. 18, which also shows the parameters used to assess F_d. A comparison of the results of the damaged areas for each cutting speed for both drilling techniques is given in Fig. 19. This confirms a significant impact of the spindle speed on F_d. Apparently, when the cutting speed is increased, the size of the damaged area is gradually decreased using CD and slightly increased using UAD, similarly to the trend for the crater depth. This means that the deepest damage also had the largest surficial area. Therefore, UAD helps to reduce both the area and depth of such damage.

4. Analytical model of UAD

The analytical model presented here describes UAD using a core drill bit with a diameter of 6 mm. In the model, a solution for a contact problem for a spherical particle was applied. Twist drill bits have non-spherical tips; thus, the modelling was performed for a core drill bit with a diamond cover. This model allowed the calculation of thrust force depending on feed rate. To compare the experimental results with the calculations, averages of the thrust force levels for the CD were used only for the initial stage of drilling, indicated as T_{av} in Fig. 11a. At this stage, the marble dust has sufficient space to collect inside the core drill bit, so that the effect of dust compaction on the cutting force is minimal. This limitation arises because the model does not consider additional factors resulting from an increase in thrust force. The result of the averaging is shown in Fig. 20.
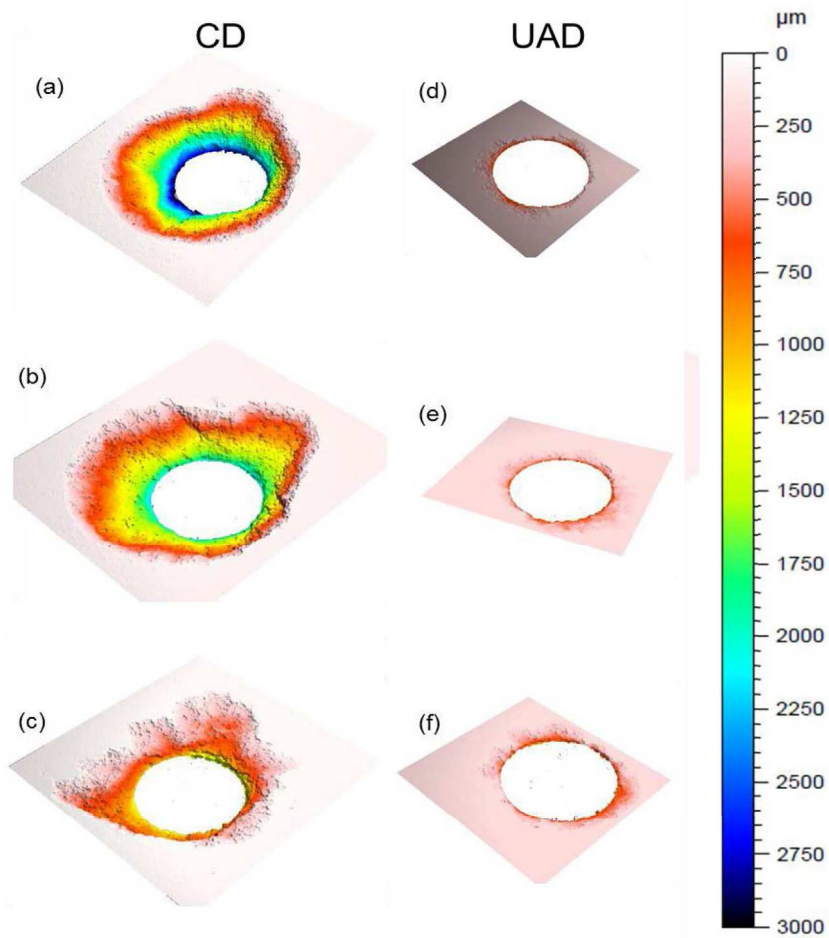
Fig. 16. Exit hole profiles for CD − (a) 85 rpm, (b) 180 rpm and (c) 260 rpm. Exit hole profiles for UAD − (d) 85 rpm, (e) 180 rpm and (f) 260 rpm.
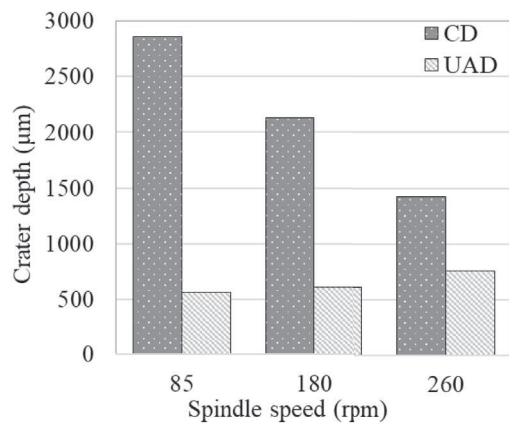

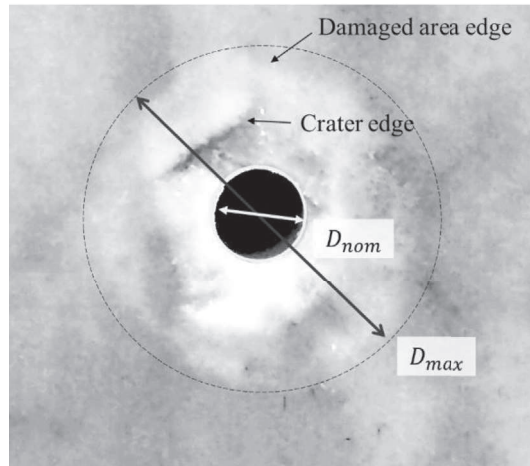**Fig. 17.** Crater depth resulting from CD and UAD at different spindle speeds.

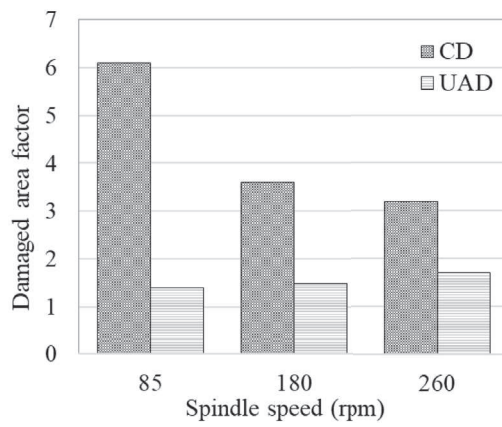**Fig. 18.** Damaged area in marble.

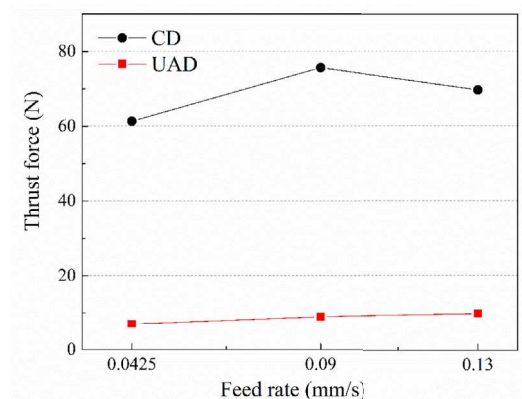**Fig. 19.** Damaged area factor in CD and UAD at different cutting speeds.

Fig. 20. CD thrust force average for interval T_{av} compared to UAD.

4.1. Energy calculations

The core drill bit used in the experiments had a diamond-covered tip, with the cutting process being performed by the diamond particles. In the analytical model of UAD, as a first step, one diamond particle was considered.

In UAD, due to the applied ultrasonic vibration, the diamond particles penetrate into the sample material at an initial speed (Fig. 21). Therefore, a solution of the Hertz contact problem, which considers the contact between a rigid sphere and an elastic half-space, could be used for the model [19].

The solution of the contact problem allows for the calculation of the radial component of the tensile stress in the contact area:

$$\sigma(t) = \frac{1 - 2\nu}{2} \frac{P(t)}{\pi a^2(t)}, \tag{1}$$

where $P(t)$ is the applied force. Taking into account the oscillating motion, the stress can be approximated as:

$$\sigma(t) = \sigma_{max} \sqrt{\sin \frac{\pi t}{t_0} (H(t) - H(t - t_0))}, \tag{2}$$

where $\sigma_{\max}$ is the critical stress, $H(t)$ is the Heaviside step function and t_0 is the contact time of the particle with the material.

In his book [1], Kumabe theoretically and experimentally demonstrated the existence of a critical cutting speed in vibration cutting, at which the tool gained constant contact with the sample. At this speed, the vibrational character of the cutting disappeared, and the regime changed to conventional cutting. The critical cutting speed is equal to $2\pi A f$, where A and f are the amplitude and frequency of the vibration. Thus, the cutting speed becomes critical when the speed of motion of the vibrating tool's edge reaches its magnitude. By analogy with vibration cutting, the presented model of UAD assumed the existence of a critical feed rate, at which the relative velocity of the edge of the drill bit would vanish. The critical feed rate was determined as $f_c = \frac{2A}{T}$, where A and T are the amplitude and period of vibration. The contact time at one vibration cycle can be written as:

$$t_0 = \frac{T}{2} + \frac{f}{f_c}\left(t_0^* - \frac{T}{2}\right), \tag{3}$$

where f is the current feed rate and t_0^* is the critical contact time equal to the vibration period. If the feed rate reaches its critical value, the contact time in each cycle becomes equal to the vibration period, $t_0 = T$, so that the tool is in continuous contact with the surface of the sample material. This implies a transition from UAD to CD.

The critical stress, $\sigma_{\max}$, used in Eq. (2), was derived based on the incubation time criterion, which includes two parameters: the incubation time of fracture τ and the static tensile strength σ_t [20,21]. The criterion can be presented in the following form:

$$\max_{t} \int_{t-\tau}^{t} \sigma(s)ds \leq \tau\sigma_t. \tag{4}$$

According to this model, fracture occurs due to the threshold energy (minimal energy that leads to failure), which can be related to the kinetic energy of the diamond particle, K. Because in UAD, fracture of the sample is caused by the impact of this particle, K can be computed from the expressions derived in Ref. [18]:
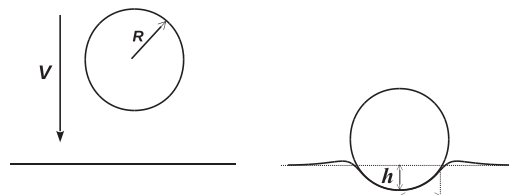

Fig. 21. Contact of diamond particle with marble sample (V – initial speed of particle, R – particle radius, h – penetration depth, a – radius of contact area).

$$K = \alpha \frac{t_0^3 \sigma_{max}^{\frac{13}{2}}}{\rho^{\frac{3}{2}} E^4},$$
(5)

where α is the dimensionless constant [18], and ρ is the free parameter with a dimension of density that determines the drilling intensity.

Since there was more than one diamond particle on the tip of the core drill bit, the parameter ρ was changed to increase the intensity of the load, thereby considering the contribution of all the particles.

4.2. Force prediction

In the developed model, the threshold fracture energy is the work of the thrust force on a displacement equal to a characteristic size, d:

$$F_c = \frac{K}{d}.$$
(6)

The values of d and of the incubation time, τ, depend on the length scale of the fracture. The incubation time reported in Table 1 was experimentally determined using the SHPB dynamic tests [27] performed using marble rods with a diameter of 20 mm and an impact impulse length of 600 mm. The characteristic size, d, was calculated as $d = 2K_{Ic}^2/\pi\sigma_t^2$, where K_{Ic} is the critical fracture toughness and σ_t is the static tensile strength [23]. Those two mechanical parameters were obtained from experiments performed at the same length scale of fracture as in the SHPB tests. However, in UAD, the sizes of the impacting diamond particles are approximately equal to 0.1 mm and, consequently, fracture occurs at a smaller (micro) scale compared to that of the SHPB tests. Thus, the parameters measured in experiments performed at the (macroscopic) laboratory scale could not be directly used in the proposed UAD model, since they correspond to a different level of fracture. A space-time model of length-scale hierarchy has been proposed [23].

The macroscopic strength parameters were converted to the microscale by exploiting the principle of equal power first proposed by Petrov et al. [22]. This principle states that the average characteristic power is constant for every fracture level, and can be written as:

$$\frac{Q_1}{\tau_1} = \frac{Q_2}{\tau_2} = const,$$
(7)

where Q_i is the activation fracture energy and τ_i is the incubation time for the ith length scale. The fracture energy in dynamic tests is equal to the elastic potential energy of a bar with a length equal to that of the impulse length:

$$Q_1 = \frac{1}{2}E\varepsilon^2 V.$$
(8)

The strain, ε, is defined as $\varepsilon = \max(\varepsilon_i - \varepsilon_r - \varepsilon_t)$, where ε_i, ε_r and ε_t are the strains of the incident, reflected and transmitted pulses, respectively. The activation fracture energy, Q_2, in the drilling is equal to the threshold energy, K (Eq. (5)). The incubation time, τ_1, is related to the fracture in dynamic tests, and is equal to τ_t (Table 1). Applying Eq. (7), the incubation time for the UAD can be computed as: $\tau_2 = 0.1$ μs. The characteristic size, d, for the microscale was assumed to be equal to the average particle size.

With all the parameters known, the thrust force can be computed from Eq. (6) for different feed rates. The resulting curve is given in Fig. 22, together with the experimental data obtained from our CD and UAD experiments for marble. The proposed theoretical model predicts an increase in thrust force with feed rate, f, up to a critical level, $f_c \approx 295$ mm/s, at which point, it assumes a constant value that corresponds to a change in drilling regime from UAD to CD. This constant force value is approximately equal to the thrust force experimentally measured from the CD experiments. Furthermore, at the lower feed rates, there was a good agreement with the UAD data.

Also, it is worth noting that the experimental results for CD showed a tendency towards increased thrust force with increased feed rate [8]. Conversely, it is known that thrust force decreases with increasing spindle speed [28]. In the presented model, it is assumed that the ratio between feed rate and spindle speed is set in such a way that the thrust force remains constant at a certain level. However, it should be noted that, due to the limitations of the drilling setup, it was not possible to test all the feed rates considered in the theoretical analysis.

5. Discussion

The results for UAD in marble show that this technique produces similar improvements (and, in some cases, is even more effective) to UAD in metals and composites. The extent of the reduction in force and torque was greater than the results
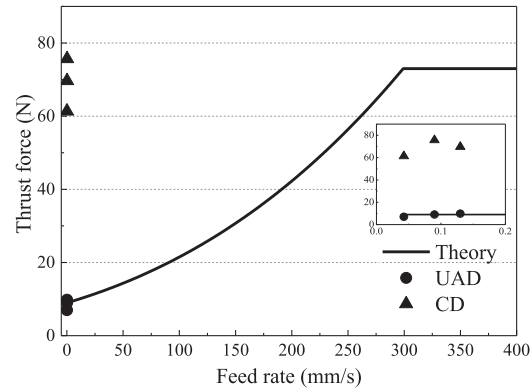
Fig. 22. Relation between feed rate and thrust force in UAD (solid line represents the theoretical calculation of UAD; circles/triangles represent the experimental data for UAD/CD).

obtained from stone drilling [11]. Thus, in general, UAD has been proved effective for brittle materials, and the results of this work can be applied to materials with mechanical properties similar to those of marble.

For the two studied twist drill bits with 3-mm diameters, the lowest thrust force was achieved using the jobber drill bit. So, if delicate processing of marble or similar materials is required, this drill bit would be preferable. However, it should be noted that the effect of ultrasound excitation disappears when using the jobber drill bit at high speeds. Therefore, for high-speed processing, a different drill bit should be used, such as the concrete drill bit.

The experiments with the core drill bit showed that UAD also effectively improved the quality of drilling, in spite of a geometric difference with the twist drill bit. It was also found that UAD with the core drill bit allowed the cutting of cylinders from the material. In the experiments, these cylinders were broken because of the small inner diameter of the drill. However, it can be assumed that, by increasing the radius of the drill bit, it would be possible to drill out a solid cylinder. This could have practical applications; for example, both dynamic (on SHPBs) and static strength tests require cylindrical samples.

The results from the analytical model correlated well with the experimental data, and also described a decrease in the efficiency of UAD with an increase in processing speed, as had been observed by Kumabe [1]. This approach also showed a good correlation with experiments on ultrasonically-assisted cutting. Consequently, the incubation-time approach is a good tool for describing the techniques of treatments using ultrasound. However, in this model, the rotational speed and friction were not explicitly specified and, therefore, the inclusion of these parameters should form one of the next stages in the development of the analytical model.

6. Conclusions

UAD, which couples ultrasonic vibration with traditional drilling methods, can be used for rock machining. It provides remarkable advantages over CD. This paper has presented experimental and theoretical investigations of both techniques. Experiments were conducted using a 6-mm-diameter core drill bit and two types of 3-mm-diameter twist drill bits. The drilling was performed on marble, and its response to the drilling was investigated, along with the advantages of using UAD. The theoretical study of UAD was based on an analytical model that would predict the thrust force of the process. The model was developed by combining the solution of a contact problem and the incubation time approach. From this study, the following results and conclusions are apparent.

1. Low forces are required to produce damage-free holes in brittle materials, such as marble. Traditional methods cannot meet this requirement. The experimental study demonstrated that UAD is able to ensure damage-free drilling in brittle materials.
2. Experiments using the masonry drill bit showed that UAD reduced thrust force and torque by an average of 45% and 54%, respectively, when compared to CD. The lowest spindle speed of 40 rpm used in the tests at a feed rate of 0.03 mm/rev showed the highest effectiveness.
3. Using the jobber drill bit resulted in lower values of thrust force and torque than using the masonry drill bit for both CD and UAD. However, with an increase in feed rate, the benefits of UAD disappeared, accompanied by a sharp jump in the force and torque to levels corresponding to those of CD. This was caused by dust compaction inside the hole and on the tool reducing the effectiveness of the vibration. So, the jobber drill bit is preferable to the masonry drill bit when drilling marble, but not above certain feed rates.

4. Compared to the other drills, CD with the core drill bit produced the highest thrust force and torque values, reaching averages of up to 252 N and 0.7 Nm, respectively. UAD, in contrast, was able to reduce these values by 93% (force) and 96% (torque).

5. Using the core drill bit, the high forces associated with CD created craters on the exit side of the sample (up to 3 mm deep). UAD contributed to a significant reduction in both the depth and area of such damage.

6. The forces computed via the analytical model for different feed rates were compared with those measured in the UAD and CD experiments, performed on marble using the core drill bit. A good agreement was found between the upper and lower force values at the experimental feed rates, thus confirming the reliability of the predictions of the model. However, for a more complete validation of the results, further experiments will be required.

Acknowledgments

References

[1] J. Kumabe, Vibration Cutting, Jikkyou Publishing Co, Tokyo, 1979.

[2] V.I. Babitsky, A.N. Kalashnikov, A. Meadows, A.A.H.P. Wijesundara, Ultrasonically assisted turning of aviation materials, J. Mater. Process. Technol. 132 (2003) 157–167, https://doi.org/10.1016/S0924-0136(02)00844-0.

[3] P.N.H. Thomas, V.I. Babitsky, Experiments and simulations on ultrasonically assisted drilling, J. Sound Vib. 308 (2007) 815–830, https://doi.org/10.1016/j.jsv.2007.03.081.

[4] A. Sanda, I. Arriola, V. Garcia Navas, I. Bengoetxea, O. Gonzalo, Ultrasonically assisted drilling of carbon fibre reinforced plastics and Ti6Al4V, J. Manuf. Process. 22 (2016) 169–176, https://doi.org/10.1016/j.jmapro.2016.03.003.

[5] B. Azarhoushang, J. Akbari, Ultrasonic-assisted drilling of inconel 738-LC, Int. J. Mach. Tool Manuf. 47 (2007) 1027–1033, https://doi.org/10.1016/j.ijmachtools.2006.10.007.

[6] Y.S. Liao, Y.C. Chen, H.M. Lin, Feasibility study of the ultrasonic vibration assisted drilling of Inconel superalloy, Int. J. Mach. Tool Manuf. 47 (2007) 1988–1996, https://doi.org/10.1016/j.ijmachtools.2007.02.001.

[7] B.V. Azghandi, M.A. Kadivar, M.R. Razfar, An experimental study on cutting forces in ultrasonic assisted drilling, Procedia CIRP 46 (2016) 563–566, https://doi.org/10.1016/j.procir.2016.04.070.

[8] F. Makhdum, V.A. Phadnis, A. Roy, V.V. Silberschmidt, Effect of ultrasonically-assisted drilling on carbon-fibre-reinforced plastics, J. Sound Vib. 333 (2014) 5939–5952, https://doi.org/10.1016/j.jsv.2014.05.042.

[9] A. Gupta, S. Barnes, I. McEwen, N. Kourra, M.A. Williams, Study of cutting speed variation in the ultrasonic assisted drilling of carbon fibre composites, in: ASME Int. Mech. Eng. Congr. Expo, ASME, 2014, p. 37046, https://doi.org/10.1115/IMECE2014-37046.

[10] V.I. Babitsky, V.K. Astashev, A. Meadows, Vibration excitation and energy transfer during ultrasonically assisted drilling, J. Sound Vib. 308 (2007) 805–814, https://doi.org/10.1016/j.jsv.2007.03.064.

[11] U. Heisel, R. Eisseler, R. Eber, J. Wallaschek, J. Twiefel, M. Huang, Ultrasonic-assisted machining of stone, Prod. Eng. 5 (2011) 587–594, https://doi.org/10.1007/s11740-011-0330-1.

[12] V.A. Phadnis, F. Makhdum, A. Roy, V.V. Silberschmidt, Experimental and numerical investigations in conventional and ultrasonically assisted drilling of CFRP laminate, Procedia CIRP 1 (2012) 455–459, https://doi.org/10.1016/j.procir.2012.04.081.

[13] M. Wiercigroch, R.D. Neilson, M.A. Player, Material removal rate prediction for ultrasonic drilling of hard materials using an impact oscillator approach, Phys. Lett. Sect. A Gen. At. Solid State Phys. 259 (1999) 91–96, https://doi.org/10.1016/S0375-9601(99)00416-8.

[14] M. Wiercigroch, J. Wojewoda, A.M. Krivtsov, Dynamics of ultrasonic percussive drilling of hard rocks, J. Sound Vib. 280 (2005) 739–757, https://doi.org/10.1016/j.jsv.2003.12.045.

[15] U. Heisel, R. Eber, J. Wallaschek, J. Twiefel, Kinematic model for ultrasonic-assisted manufacturing of bore holes with undefined cutting edges, Adv. Mater. Res. 223 (2011) 794–803, https://doi.org/10.4028/www.scientific.net/amr.223.794.

[16] N. Qin, Z.J. Pei, C. Treadwell, D.M. Guo, Physics-based predictive cutting force model in ultrasonic-vibration-assisted grinding for titanium drilling, J. Manuf. Sci. Eng. 131 (2009), 041011, https://doi.org/10.1115/1.3159050.

[17] D. Liu, W.L. Cong, Z.J. Pei, Y. Tang, A cutting force model for rotary ultrasonic machining of brittle materials, Int. J. Mach. Tool Manuf. 52 (2011) 77–84, https://doi.org/10.1016/j.ijmachtools.2011.09.006.

[18] N.A. Gorbushin, G.A. Volkov, Y.V. Petrov, Simulation of the behavior of the cutting force during ultrasonic rotary machining of materials using structure-time fracture mechanics, Tech. Phys. 59 (2014) 852–856, https://doi.org/10.1134/s1063784214060103.

[19] K. Johnson, Contact Mechanics, Cambridge University Press, 1985.

[20] Y.V. Petrov, N.F. Morozov, On the modeling of fracture of brittle solids, J. Appl. Mech. 61 (1994) 710–713, https://doi.org/10.1115/1.2901518.

[21] Y.V. Petrov, N.F. Morozov, V.I. Smirnov, Structural macromechanics approach in dynamics of fracture, Fatigue Fract. Eng. Mater. Struct. 26 (2003) 363–372, https://doi.org/10.1046/j.1460-2695.2003.00602.x.

[22] Y.V. Petrov, A.A. Gruzdkov, N.F. Morozov, The principle of equal powers for multilevel fracture in continua, Dokl. Phys. 50 (2005) 448–451, https://doi.org/10.1134/1.2074112.

[23] Y. V Petrov, B.L. Karihaloo, V. V Bratov, A.M. Bragov, Multi-scale dynamic fracture model for quasi-brittle materials, Int. J. Eng. Sci. 61 (2012) 3–9, https://doi.org/10.1016/j.ijengsci.2012.06.004.

[24] H. Kolsky, An investigation of the mechanical properties of materials at very high rates of loading, Proc. Phys. Soc. Sect. B 62 (1949) 676–700, https://doi.org/10.1088/0370-1301/62/11/302.

[25] K. Xia, W. Yao, Dynamic rock tests using split Hopkinson (Kolsky) bar system − a review, J. Rock Mech. Geotech. Eng. 7 (2015) 27–59, https://doi.org/10.1016/J.JRMGE.2014.07.008.

[26] M.M. Elbeblawi, M.A. Sayed, G.Y. Boghdadi, H.H. Hamd_Allh, Using diamond core bit to determine the suitable operating parameters in drilling some marble rocks, J. Eng. Sci. 41 (2013) 723–745.

[27] S.N. Verichev, I.V. Smirnov, Y.V. Petrov, A.M. Bragov, G.A. Volkov, A.K. Abramian, Dynamic failure of dry and fully saturated limestone samples based on incubation time concept, J. Rock Mech. Geotech. Eng. 9 (2016) 125–134, https://doi.org/10.1016/j.jrmge.2016.09.004.

[28] H. Paktinat, S. Amini, Numerical and experimental studies of longitudinal and longitudinal-torsional vibrations in drilling of AISI 1045, Int. J. Adv. Manuf. Technol. 94 (2018) 2577–2592, https://doi.org/10.1007/s00170-017-0893-x.